ORIGINAL ARTICLE

The Genetic Evolution of Melanoma from Precursor Lesions

A. Hunter Shain, Ph.D., Iwei Yeh, M.D., Ph.D., Ivanka Kovalyshyn, D.O., Aravindhan Sriharan, M.D., Eric Talevich, Ph.D., Alexander Gagnon, B.A., Reinhard Dummer, M.D., Jeffrey North, M.D., Laura Pincus, M.D., Beth Ruben, M.D., William Rickaby, M.B., Ch.B., Corrado D'Arrigo, M.B., Ch.B., Ph.D., Alistair Robson, F.R.C.Path., and Boris C. Bastian, M.D.

ABSTRACT

BACKGROUND

The pathogenic mutations in melanoma have been largely catalogued; however, the order of their occurrence is not known.

METHODS

We sequenced 293 cancer-relevant genes in 150 areas of 37 primary melanomas and their adjacent precursor lesions. The histopathological spectrum of these areas included unequivocally benign lesions, intermediate lesions, and intraepidermal or invasive melanomas.

RESULTS

Precursor lesions were initiated by mutations of genes that are known to activate the mitogen-activated protein kinase pathway. Unequivocally benign lesions harbored *BRAF* V600E mutations exclusively, whereas those categorized as intermediate were enriched for *NRAS* mutations and additional driver mutations. A total of 77% of areas of intermediate lesions and melanomas in situ harbored *TERT* promoter mutations, a finding that indicates that these mutations are selected at an unexpectedly early stage of the neoplastic progression. Biallelic inactivation of *CDKN2A* emerged exclusively in invasive melanomas. *PTEN* and *TP53* mutations were found only in advanced primary melanomas. The point-mutation burden increased from benign through intermediate lesions to melanoma, with a strong signature of the effects of ultraviolet radiation detectable at all evolutionary stages. Copy-number alterations became prevalent only in invasive melanomas. Tumor heterogeneity became apparent in the form of genetically distinct subpopulations as melanomas progressed.

CONCLUSIONS

Our study defined the succession of genetic alterations during melanoma progression, showing distinct evolutionary trajectories for different melanoma subtypes. It identified an intermediate category of melanocytic neoplasia, characterized by the presence of more than one pathogenic genetic alteration and distinctive histopathological features. Finally, our study implicated ultraviolet radiation as a major factor in both the initiation and progression of melanoma. (Funded by the National Institutes of Health and others.)

From the Departments of Dermatology and Pathology (A.H.S., I.Y., E.T., A.G., J.N., L.P., B.R., B.C.B.) and the Helen Diller Family Comprehensive Cancer Center (A.H.S., I.Y., E.T., A.G., B.C.B.), University of California, San Francisco (UCSF), San Francisco; the Departments of Dermatology and Pathology, Cleveland Clinic, Cleveland (I.K.); the Department of Pathology, Orlando Health, Orlando, FL (A.S.); the Department of Dermatology, University Hospital of Zurich, Zurich, Switzerland (R.D.); and the Department of Dermatology, Dorset County Hospital, Dorchester (C.D.), and the Department of Dermatology, St. John's Institute of Dermatology, London (W.R., A.R.) — both in the United Kingdom. Address reprint requests to Dr. Bastian at the UCSF Dermatopathology Service, 1701 Divisadero St., Suite 280, San Francisco, CA 94115, or at boris.bastian@ucsf.edu.

N Engl J Med 2015;373:1926-36.
DOI: 10.1056/NEJMoa1502583

Cancer arises through the accumulation of genetic alterations that lead to unrestrained cell proliferation. Large-scale sequencing projects that catalogue mutations in melanoma have been carried out mostly on advanced tumors, so it is difficult to infer the order of mutations. Melanomas often arise from distinctive precursor lesions such as melanocytic nevi, intermediate lesions, or melanoma in situ, which makes the analysis of their progression possible.

The succession of genetic alterations that leads to melanoma is incompletely understood. Somatic mutations in dominant melanoma oncogenes such as *BRAF*, *NRAS*, *GNAQ*, or *GNA11* and rearrangements resulting in fusion kinases are already present in benign nevi, indicating that they occur early during progression.[1-6] However, little is known about the sequential order of additional mutations that are present in late-stage melanomas, including mutations of *TERT*, *CDKN2A*, *TP53*, genes encoding SWI/SNF subunits (most commonly *ARID2*), and *PTEN*, among others.[7-14]

There has been a long-standing debate about the existence of an intermediate category of lesions between clearly benign nevi and melanoma. This is exemplified by the concept of dysplastic nevi, which has remained controversial.[15] Delineating the order of genetic alterations that lead to primary melanomas and linking their emergence to specific progression stages of the primary lesion could yield biomarkers that would improve diagnosis and prognostication, because such biomarkers would allow the determination of how far a given melanocytic neoplasm has evolved. A better understanding of the genetic evolution of melanoma could also clarify the existence of intermediate lesions, because they would be predicted to have more pathogenic mutations than benign lesions but fewer than unequivocal melanomas.

METHODS

CASES

A total of 37 formalin-fixed, paraffin-embedded (FFPE) melanocytic neoplasms, enriched for melanomas with histologically distinct precursors, were retrieved from the archives of the Dermatopathology Sections of the University of California, San Francisco; St. John's Hospital in London; and the University Hospital of Zurich. In total, 150 distinct areas were manually microdissected for sequencing (see Supplementary Appendix 2, available with the full text of this article at NEJM.org). Each area was independently assessed by eight dermatopathologists and grouped into one of the following histologic categories: benign, intermediate but probably benign, intermediate but probably malignant, or melanoma. The American Joint Committee on Cancer staging system was used to further stratify melanomas.

SEQUENCING

For each sample, 25 to 250 ng of DNA was prepared for sequencing with the use of the NuGEN Ovation or Bioo Scientific NEXTflex library preparation kits according to the manufacturer's instructions. Formalin fixation and the small number of cells in many cases resulted in reduced complexity of sequencing libraries with high fractions of duplicate reads, as has been described previously for similar samples.[16-21] To achieve the desired sequencing depth of unique reads, we elected to perform targeted sequencing of 293 cancer genes (see Supplementary Appendix 3). We also analyzed the entire exomes of all microdissected samples from two cases with the highest library complexities and did not identify relevant genetic alterations outside the 293-gene footprint.

DATA ANALYSIS

Sequencing reads were mapped and groomed with the use of Burrows–Wheeler Aligner, Genome Analysis Toolkit, and Picard (http://broadinstitute.github.io/picard/). Copy number was inferred with the use of CNVkit.[22] Neoplastic cellularity was estimated from the frequencies of somatic and germline variant alleles. Phylogenetic trees were constructed manually according to the principles of maximum parsimony and were rooted at the germline state. Additional details can be found in Supplementary Appendix 1.

RESULTS

GENETIC EVOLUTION FROM PRECURSORS TO MELANOMA

We obtained an average sequencing coverage of 281× for the 150 samples, which enabled us to identify somatic mutations even in the presence of a high level of stromal-cell contamination

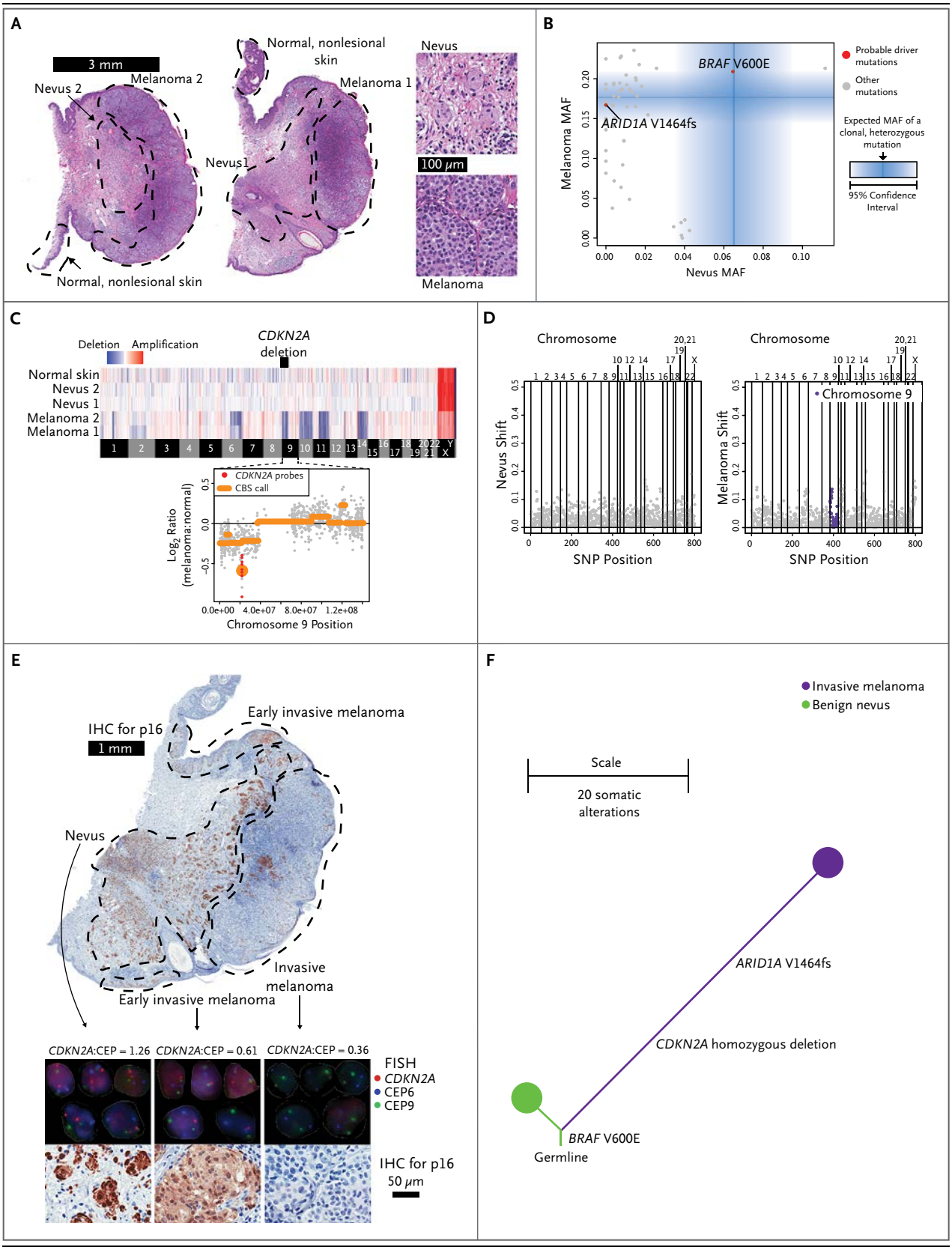

Figure 1 (facing page). The Genetic Evolution of Melanoma from a Precursor Nevus (Case 31).

Panel A shows hematoxylin and eosin–stained sections of normal, nonlesional skin, two areas of benign nevus, and two areas of the invasive melanoma that were microdissected as indicated. Panel B shows a scatterplot of mutant allele frequencies (MAFs) in the nevus areas as compared with the melanoma areas. The blue lines correspond to the expected allelic frequency of a clonal, heterozygous mutation after we accounted for stromal-cell contamination, with shading showing confidence intervals. In Panel C, the heatmap depicts copy-number decreases (blue) and increases (red) for each sample (rows) across the genome, with chromosome boundaries annotated. The inset scatterplot shows bin-wise copy number (gray data points); segments called with the use of the circular binary segmentation (CBS) algorithm are overlayed in orange. The bins overlapping with *CDKN2A* are indicated in red. In Panel D, the deviation from the expected allelic ratio of 0.5:0.5 of germline heterozygous single-nucleotide polymorphisms (SNPs) is plotted on the y axis and ordered by the position of each SNP across the genome on the x axis. Loss of heterozygosity of chromosome 9 (*CDKN2A*) is indicated in purple. As shown in Panel E, fluorescence in situ hybridization (FISH) and immunohistochemical analysis (IHC) for p16 antibody confirmed a stepwise decrease in *CDKN2A* relative to a control probe and a stepwise decrease in p16 at the transition to melanoma. CEP denotes centromere enumeration probe. Panel F shows the inferred evolution of Case 31.

(average, 64%; range, 15 to 90) (Supplementary Appendix 2). We compared mutations and copy-number changes among the microdissected areas, sampling multiple instances of histologically similar areas as replicates whenever feasible. A representative example is shown in Figure 1, in which normal, nonlesional tissue was microdissected along with two replicate areas of a nevus and two replicate areas of a melanoma (see Fig. S1 through S36 in Supplementary Appendix 1 for all other cases). For the most part, histologic replicates were genetically indistinguishable and were combined for analysis as in the example case (Fig. 1), with exceptions indicated (e.g., Case 25, shown in Fig. S25 in Supplementary Appendix 1).

For each case, the mutant allele frequencies of all somatic mutations were plotted for the precursor and descendant neoplasms (Fig. 1B). Fully clonal mutations that were seen in both the precursor and descendant neoplasms probably occurred early and thus included mutations that both initiated neoplastic proliferation and were propagated to the more advanced stage or stages. Therefore, the nevus in the example case was probably initiated by a *BRAF* V600E mutation (Fig. 1B). In every case, a mutation known to activate the mitogen-activated protein kinase (MAPK) signaling pathway, usually in *BRAF* or *NRAS*, could be nominated as the putative initiating oncogene (Fig. S1 through S36 in Supplementary Appendix 1).

The descendant neoplasms usually harbored additional mutations that were not present in their precursors and that therefore probably occurred later and included mutations that contributed to progression. The melanoma in the example case (Fig. 1B) probably progressed after acquiring a disabling frame-shift mutation in the tumor suppressor *ARID1A*. Progression mutations found in other cases commonly affected the *TERT* promoter (Fig. S2, S3, S9, S21, S25, and S27 in Supplementary Appendix 1), *CDKN2A* (Fig. S6, S16, S27, S33, S34, and S36 in Supplementary Appendix 1), and genes encoding SWI/SNF subunits (Fig. S1, S4, S14, S15, S21, and S22 in Supplementary Appendix 1). The presence or absence of mutations in the *TERT* promoter could not be assessed for eight cases (listed in Supplementary Appendix 2) that were analyzed before the identification of the *TERT* promoter as a mutational hotspot.[9,10]

Genomic regions affected by copy-number alterations were identified from deviations in read depth from a reference pool of normal tissues. In the example case (Fig. 1C), both areas of the nevus showed no copy-number alterations, whereas the two areas of the melanoma showed concordant losses of the short arm of chromosome 9 with a superimposed homozygous deletion including *CDKN2A*. As in the example case, copy-number alterations were infrequent in benign precursors but common in descendant neoplasms. Copy-number alterations that were associated with progression in other cases included deletions of *CDKN2A* (Fig. S2, S4, S7, S8, S13, S14, S15, S19, S21, S22, S25, S27, S29, S31, S32, and S35 in Supplementary Appendix 1), deletions of *PTEN* (Fig. S6, S8, S25, and S28 in Supplementary Appendix 1), chromosome 7q gains that increased gene dosage of mutant *BRAF* (Fig. S4, S23, and S35 in Supplementary Appendix 1), and focused amplifications of *MDM2* (Fig. S11 in Supplementary Appendix 1), *TERT* (Fig. S31 in

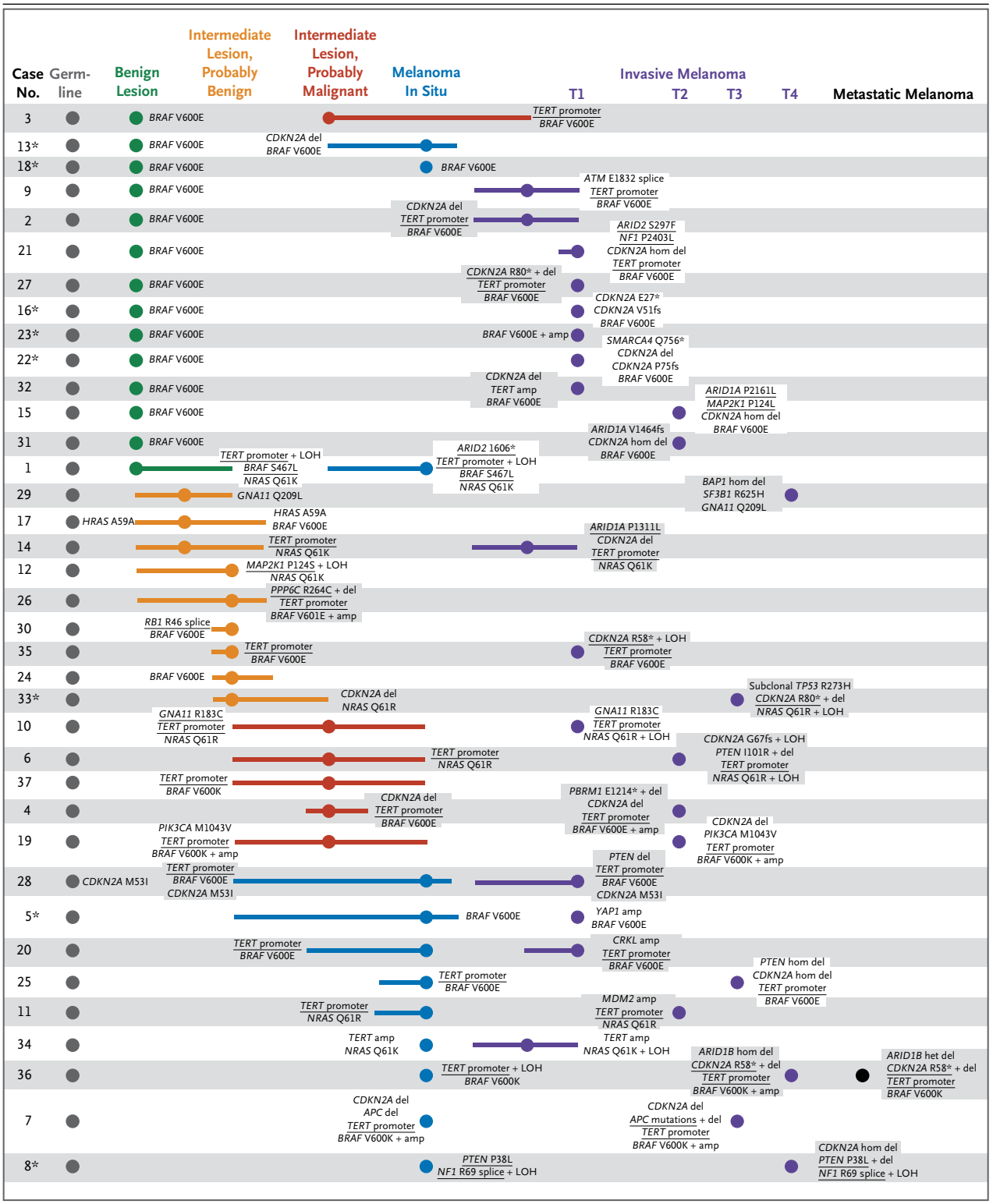

Supplementary Appendix 1) and *YAP1* (Fig. S5 in Supplementary Appendix 1).

Copy-number alterations introduce allelic imbalances of germline heterozygous single-nucleotide polymorphisms, which are evident as deviations from the expected allelic ratio of 0.5:0.5.

Figure 2 (facing page). The Genetic Evolution of All Cases.

The median (colored circle) and interquartile range (colored line) of histopathological evaluations are displayed for each area, with respective oncogenic alterations superimposed. Cases are ordered according to the stage at diagnosis for the precursor lesion. In two cases, a pathogenic mutation was present in the germline. The *TERT* promoter was not sequenced for the eight cases denoted with an asterisk. Underlined oncogenic alterations exhibited an ultraviolet-radiation–induced mutational signature. Amp denotes amplification, del deletion, fs frame shift, het heterozygous, hom homozygous, and LOH loss of heterozygosity. See Figures S1 through S36 in Supplementary Appendix 1 for a detailed description of each case.

This is exemplified in the allelic imbalance caused by the deletion of one copy of chromosome 9p in the melanoma area of the example case (Fig. 1D). Allelic imbalances served as independent validation of copy-number calls for all cases (Fig. S1 through S36 in Supplementary Appendix 1) but also identified regions of copy-number–neutral loss of heterozygosity. Copy-number–neutral loss of heterozygosity did not occur in the example case but was observed in other cases, resulting in homozygosity of mutated tumor suppressors (Fig. S6, S8, and S34 in Supplementary Appendix 1) or increased gene dosage of oncogenic alleles (Fig. S1, S6, S7, S10, S27, S34, and S35 in Supplementary Appendix 1).

Whenever feasible, we also attempted to obtain independent validation of relevant alterations by means of immunohistochemical testing, fluorescence in situ hybridization (FISH), or both (Fig. 1E; and Fig. S8, S13, S14, S15, S16, S21, S22, S23, S27, S31, S32, and S34 in Supplementary Appendix 1). As shown in Figure 1E, FISH confirmed an intact *CDKN2A* locus with robust protein expression in the nevus areas and complete loss of expression in the melanoma areas with homozygous deletion. The flanking areas of early invasive melanoma, which were not analyzed separately by means of sequencing, showed a hemizygous deletion on FISH, with corresponding intermediate levels of protein (Fig. 1E).

We partitioned genetic alterations between precursor and descendant neoplasms to deduce the phylogenetic history of each case. Shared genetic alterations constituted the trunk of the phylogenetic tree, whereas private alterations defined the branches. The lengths of trunk and branches were scaled on the basis of the number of somatic mutations, as in the example case (Fig. 1F).

CORRELATION OF MUTATION PATTERNS WITH HISTOPATHOLOGICAL FEATURES

Many melanocytic neoplasms can be classified as benign or malignant with a high degree of interobserver agreement. However, there is a gray zone of intermediate lesions that are characterized by overlapping morphologic criteria and lower interobserver agreement. It is currently unknown whether such lesions represent true biologic entities or merely reflect the limitations of histopathological assessment. Figure 2 shows the median and interquartile range of the observer evaluations for the separate areas from each case. As expected, there was a high degree of interobserver agreement at the ends of the spectrum, with a wider range in the intermediate categories.

All 13 areas that were unanimously considered to be benign showed a *BRAF* V600E mutation as the only apparent pathogenic mutation (Fig. 2). By contrast, 19 of the 21 areas classified as intermediate by at least two observers showed multiple pathogenic mutations. The intermediate lesions had a broader spectrum of initiating oncogenes than the unequivocally benign lesions, including *BRAF* V600K or K601E and *NRAS* mutations (Fig. 2 and 3A). The intermediate lesions also had a higher mutational burden than benign lesions ($P=0.03$ by Wilcoxon rank-sum test) (Fig. 3B). These findings indicate that the majority of intermediate lesions that were classified on morphologic grounds also had genetic characteristics that reside between benign and malignant neoplasms.

Among melanomas, the frequency of specific mutations, patterns of copy-number alterations, and mutational burden vary significantly with tissue and anatomical site of origin, age at diagnosis, and cumulative sun exposure, which has led to the recognition that melanomas comprise biologically distinct subtypes.[5,11] Specifically, melanomas with *BRAF* V600E mutations are more common on intermittently sun-damaged skin of younger patients and have distinct histopathological features,[24] whereas melanomas with *NRAS* mutations and *BRAF* V600K or K601E mutations occur predominantly on chronically sun-damaged skin of older patients.[25] We also observed two different modes of progression, a finding consis-

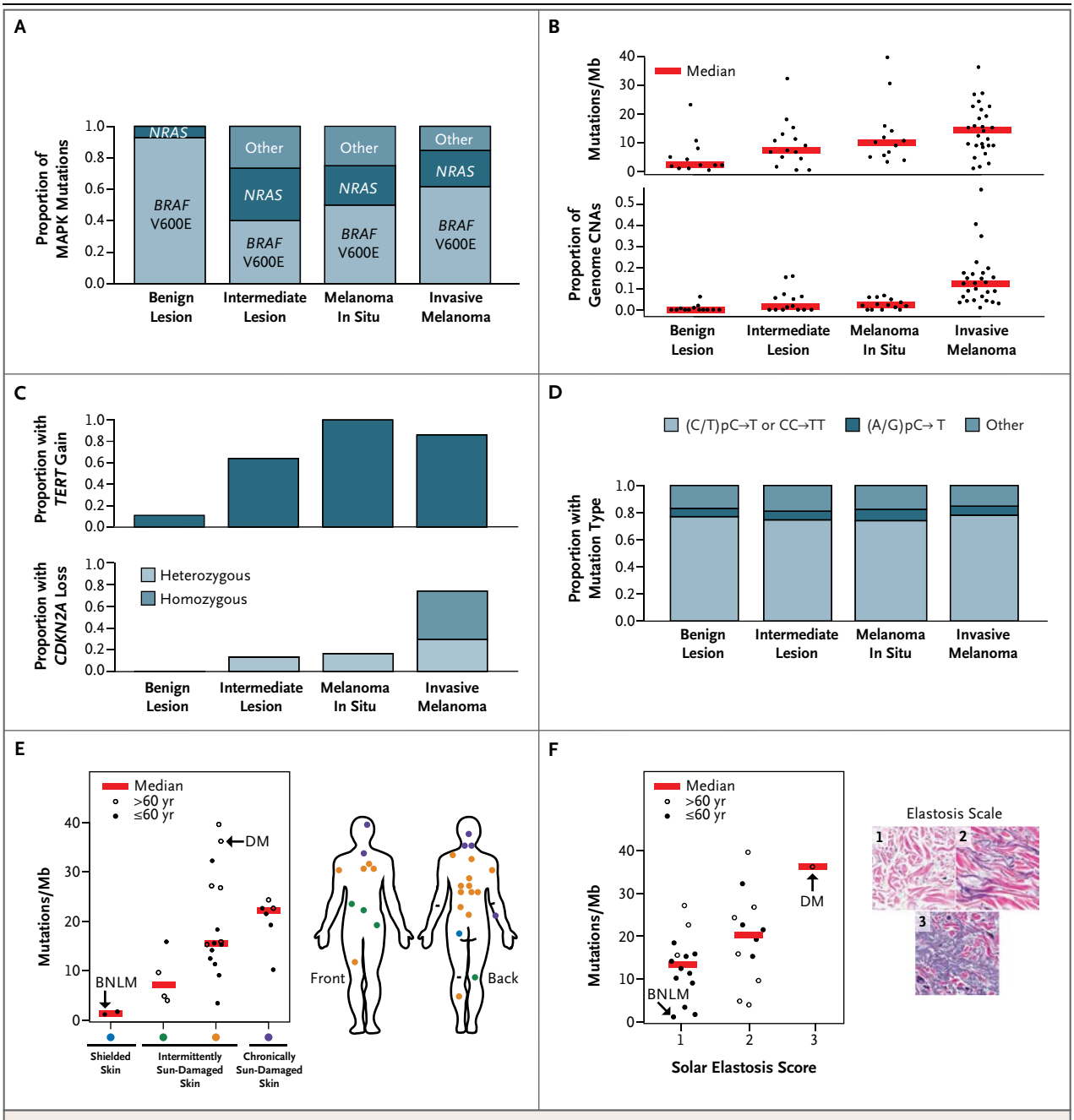

Figure 3. Patterns of Mutations and Mutation Burden at Each Stage of Progression.

Panel A shows the distribution of mitogen-activated protein kinase (MAPK) pathway mutations, with stratification according to histologic stage. Panel B shows the point-mutation burden, as measured by mutations per megabase (Mb), and the burden of copy-number alterations (CNAs), as measured by the proportion of the genome altered. Panel C shows the distribution of *TERT* and *CDKN2A* alterations by CNAs or mutations. Panel D shows the proportion of point mutations that were induced by ultraviolet radiation ([C/T]C to T). Panels E shows the correlation between mutational burden in melanoma areas and sun exposure, as inferred from the age of the patient and the anatomical site, and Panel F shows the same correlation as inferred from solar elastosis. Anatomical sites were grouped on the basis of sun exposure, as shown on the right side of Panel E. Solar elastosis was scored as described previously,[23] with examples on the right side of Panel F. BNLM denotes blue nevus–like melanoma, and DM desmoplastic melanoma.

tent with the diverging features of the lesions. Melanomas with *BRAF* V600E mutations arose from benign nevi. By contrast, melanomas with *NRAS* mutations or *BRAF* V600K or K601E mutations were more commonly associated with intermediate lesions or melanomas in situ that had already accumulated other pathogenic mutations.

Two outlier cases in terms of cumulative sun exposure further support the notion that the different melanoma subtypes show distinct progression trajectories. Case 29 was a blue nevus that progressed to a blue nevus–like melanoma (Fig. S29 in Supplementary Appendix 1), a sun-shielded melanoma subtype that is genetically related to uveal melanoma.[1,6,26] The nevus was initiated by a *GNA11* Q209L mutation as the only detectable mutation, and progression to melanoma coincided with a subsequent *SF3B1* R625H mutation and homozygous loss of *BAP1*. There were very few point mutations in the blue nevus–like melanoma, and they did not exhibit damage induced by ultraviolet radiation. Case 8 was a melanoma in situ that was associated with desmoplastic melanoma (Fig. S8 in Supplementary Appendix 1), a biologically distinct subtype of melanoma that is associated with high cumulative sun exposure and characterized by sarcomatous growth patterns.[27] The earliest detectable pathogenic mutation was a homozygous splice-site mutation of *NF1* that was already present in the in situ area, and progression to desmoplastic melanoma coincided with homozygous loss of *CDKN2A* and *PTEN*. There were numerous point mutations reflective of ultraviolet radiation, a finding that is consistent with the high sun exposure associated with most desmoplastic melanomas.[28]

Despite differences in initiating oncogenes, there were strong similarities among the later mutations that accumulated during subsequent stages of progression. *TERT* promoter mutations emerged early in intermediate lesions and melanomas in situ, occurring in 77% of these neoplasms (Fig. 3C). Loss of both *CDKN2A* copies was evident exclusively in invasive melanomas (Fig. 3C). Mutations in SWI/SNF chromatin remodeling genes also emerged predominantly in invasive melanomas (Fig. 2). Finally, losses of *PTEN* and *TP53* were uncommon in our series but occurred exclusively in thicker, invasive melanomas (Fig. 2), findings that imply that these mutations may occur later.

MUTATIONAL PATTERNS DURING MELANOMA EVOLUTION

The burden of point mutations escalated with each histologic stage (Fig. 3B), and the mutations exhibited a signature of the effects of ultraviolet radiation across all progression stages (Fig. 3D). In the melanoma areas, the burden of point mutations correlated with cumulative sun exposure as inferred clinically (Fig. 3E) and histologically (Fig. 3F). Copy-number alterations were rare in unequivocally benign lesions and were present only occasionally in intermediate lesions and melanomas in situ (Fig. 3B). In contrast, invasive melanomas invariably harbored copy-number alterations, affecting larger portions of the genome. In aggregate, these results suggest that ultraviolet radiation is a dominant mutagen in the pathogenesis of sun-exposed melanomas that acts throughout all stages of progression, starting with the initiation of precursor lesions, whereas chromosomal instability arises as an additional factor at the transition to the invasive stage.

The distribution of genetic alterations, point mutations, and copy-number changes among different areas of individual cases revealed the phylogenetic history of each neoplasm. Melanocytic neoplasms evolved linearly during the earliest stages and exhibited branched evolution as they became more advanced (Fig. S37 in Supplementary Appendix 1).

DISCUSSION

From our data comparing individual primary melanomas with melanoma precursor lesions at distinct pathologic levels in different patients, we inferred a stereotypical pattern of melanoma evolution (Fig. 4). Given that an individual tumor cannot readily be studied as it progresses from benign to malignant, our approach nevertheless appeared to reveal a more or less consistent pattern of genetic changes. The progression cascade was initiated by mutations known to activate the MAPK pathway, which were followed by activation of telomerase and disruption of the G1–S checkpoint. The mutational signatures implicated ultraviolet radiation as a dominant pathogenic factor

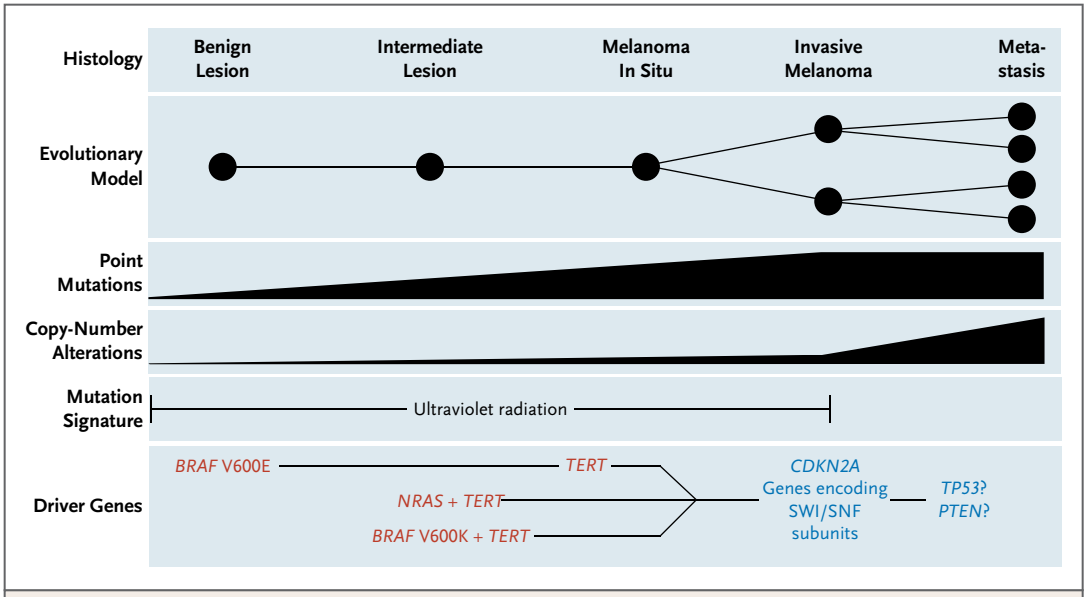

Figure 4. Proposed Models for Progression of Melanomas Developing on Sun-Exposed Sites.

that acts from nevogenesis throughout the more advanced histologic stages. The pathogenic role of ultraviolet radiation was further supported by the ultraviolet-radiation–induced mutational signature of several driver mutations (Fig. 2). In aggregate, these findings indicate that sun protection should reduce melanoma risk, especially among persons with a high nevus count.

Our study indicates that different melanoma subtypes evolve through distinct trajectories. All unequivocally benign lesions harbored *BRAF* V600E as the only apparent pathogenic alteration. Although we did not survey the entire genome, we did sequence every bona fide melanoma gene that was nominated from large-scale exome studies,[7,8] and the absence of additional driver mutations implies that *BRAF* V600E is sufficient to form a nevus. By contrast, and unexpectedly, every precursor lesion with *NRAS* or other *BRAF* mutations harbored additional oncogenic alterations, and these lesions fell into the intermediate category. The biologic differences between benign and intermediate precursors most likely reflect the divergent evolutionary paths of melanomas on skin with chronic sun-induced damage and melanomas on skin without such damage.[29-31] The distinctive evolution of the blue nevus–like melanoma and the desmoplastic melanoma further support the notion that different subtypes of melanomas have distinct evolutionary trajectories.

The existence of a category of lesions residing between clearly benign and clearly malignant states has long been proposed but has remained controversial. The term "dysplastic nevus" was introduced to describe the enlarged acquired nevi that are often found in patients who have a genetic predisposition to melanoma.[32] The clinical phenotype of multiple dysplastic nevi has been shown to be a reliable predictor of melanoma risk.[33,34] However, the relevance of the histopathological features that are attributed to dysplastic nevi has remained controversial, and there is considerable variation in the way in which dysplastic nevi are diagnosed and managed clinically.[15] We therefore avoided the term "dysplastic" in grading individual areas and instead asked the participating pathologists to assign each lesion a probability of malignancy. Intermediate lesions showed discrete genetic alterations, which indicated that they were biologically distinct. However, detailed follow-up studies will be necessary to specifically delineate their histopathological characteristics and determine whether genetic or morphologic features can be identified that determine the risk of their progression to melanoma.

TERT promoter mutations were the earliest secondary alterations, already emerging in intermediate lesions and melanomas in situ (Fig. 4). The number of cells in these comparatively pauci-

cellular neoplasms makes it surprising that a genetic alteration that bypasses replicative senescence underwent positive selection. The early emergence of *TERT* mutations suggests that the cells in these lesions are or have been dividing rather than senescent, with proliferation counterbalanced by attritional factors, such as a cytotoxic immune response or cell death or cell-cyle arrest due to mitotic errors as a consequence of replicative stress.[35] This model predicts that once the cells of a precursor exhaust their replicative potential, this balance would tip in favor of cell attrition and result in involution, a well-documented fate of acquired nevi later in the patient's life.[36] By contrast, precursors that acquired *TERT* mutations would persist and could acquire subsequent mutations, with progression toward melanoma.

We found that melanocytic neoplasms transitioned from linear to branched evolution at later stages of progression, leading to tumor heterogeneity. Polyclonal neoplasms are expected to be more resilient to intrinsic defenses of the immune system and to therapeutic approaches, which may explain the therapeutic success of early removal.

In summary, our study defined the succession of genetic alterations during melanoma progression and can serve as the foundation for formulation of refined criteria for diagnosis and prognostication. It revealed an intermediate category of melanocytic neoplasia, characterized by the presence of more than one pathogenic genetic alteration — a finding that helps to resolve the decades-long controversy about dysplastic nevi. Finally, our study implicated ultraviolet radiation as a major factor in both the initiation and progression of melanoma.

Supported by grants (R01-CA131524, P01 CA025874, and 5T32CA177555-02) from the National Institutes of Health, and the Gerson and Barbara Bass Bakar Distinguished Professorship in Cancer Research.

Disclosure forms provided by the authors are available with the full text of this article at NEJM.org.

We thank Swapna Vemula and others at the University of California, San Francisco, Dermatopathology Service for technical assistance in performing fluorescence in situ hybridization, immunohistochemical testing, tissue sectioning, and slide imaging.

REFERENCES

1. Van Raamsdonk CD, Bezrookove V, Green G, et al. Frequent somatic mutations of GNAQ in uveal melanoma and blue naevi. Nature 2009;457:599-602.
2. Wiesner T, He J, Yelensky R, et al. Kinase fusions are frequent in Spitz tumours and spitzoid melanomas. Nat Commun 2014;5:3116.
3. Pollock PM, Harper UL, Hansen KS, et al. High frequency of BRAF mutations in nevi. Nat Genet 2003;33:19-20.
4. Carr J, Mackie RM. Point mutations in the N-ras oncogene in malignant melanoma and congenital naevi. Br J Dermatol 1994;131:72-7.
5. Bastian BC. The molecular pathology of melanoma: an integrated taxonomy of melanocytic neoplasia. Annu Rev Pathol 2014;9:239-71.
6. Van Raamsdonk CD, Griewank KG, Crosby MB, et al. Mutations in *GNA11* in uveal melanoma. N Engl J Med 2010;363:2191-9.
7. Hodis E, Watson IR, Kryukov GV, et al. A landscape of driver mutations in melanoma. Cell 2012;150:251-63.
8. Krauthammer M, Kong Y, Ha BH, et al. Exome sequencing identifies recurrent somatic RAC1 mutations in melanoma. Nat Genet 2012;44:1006-14.
9. Horn S, Figl A, Rachakonda PS, et al. TERT promoter mutations in familial and sporadic melanoma. Science 2013;339:959-61.
10. Huang FW, Hodis E, Xu MJ, Kryukov GV, Chin L, Garraway LA. Highly recurrent TERT promoter mutations in human melanoma. Science 2013;339:957-9.
11. Curtin JA, Fridlyand J, Kageshita T, et al. Distinct sets of genetic alterations in melanoma. N Engl J Med 2005;353:2135-47.
12. Harbour JW, Roberson EDO, Anbunathan H, Onken MD, Worley LA, Bowcock AM. Recurrent mutations at codon 625 of the splicing factor SF3B1 in uveal melanoma. Nat Genet 2013;45:133-5.
13. Martin M, Maßhöfer L, Temming P, et al. Exome sequencing identifies recurrent somatic mutations in EIF1AX and SF3B1 in uveal melanoma with disomy 3. Nat Genet 2013;45:933-6.
14. Shain AH, Pollack JR. The spectrum of SWI/SNF mutations, ubiquitous in human cancers. PLoS One 2013;8(1):e55119.
15. Duffy K, Grossman D. The dysplastic nevus: from historical perspective to management in the modern era. Part I: historical, histologic, and clinical aspects. J Am Acad Dermatol 2012;67(1):1.e1-1.e16.
16. Kerick M, Isau M, Timmermann B, et al. Targeted high throughput sequencing in clinical cancer settings: formaldehyde fixed-paraffin embedded (FFPE) tumor tissues, input amount and tumor heterogeneity. BMC Med Genomics 2011;4:68.
17. Palescandolo E, Jones R, Raza A, et al. Can DNA from archived formalin-fixed paraffin embedded (FFPE) cancer tissues be used for somatic mutation analysis in next generation sequencing. Cancer Res 2012;72:Suppl:3178. abstract.
18. Wagle N, Berger MF, Davis MJ, et al. High-throughput detection of actionable genomic alterations in clinical tumor samples by targeted, massively parallel sequencing. Cancer Discov 2012;2:82-93.
19. Raterman D, Jefferson K, Wendt J, Brockman M, Burgess D. Target enrichment protocol for preparing formalin-fixed paraffin embedded (FFPE) tissue samples for next-generation sequencing. SeqCap EZ Library: application note. 2013 (http://www.nimblegen.com/products/lit/07180748001_FFPE_ApplicationNote_12092013.pdf).
20. Won HH, Scott SN, Brannon AR, Shah RH, Berger MF. Detecting somatic genetic alterations in tumor specimens by exon capture and massively parallel sequencing. J Vis Exp 2013;80:e50710.
21. Hedegaard J, Thorsen K, Lund MK, et al. Next-generation sequencing of RNA and DNA isolated from paired fresh-frozen and formalin-fixed paraffin-embedded samples of human cancer and normal tissue. PLoS One 2014;9(5):e98187.
22. Talevich E, Shain AH, Bastian BC. CNVkit: copy number detection and visualization for targeted sequencing using off-target reads. BioRxiv, 2014 (http://biorxiv.org/content/early/2014/10/29/010876).
23. Landi MT, Bauer J, Pfeiffer RM, et al. MC1R germline variants confer risk for

BRAF-mutant melanoma. Science 2006; 313:521-2.
24. Viros A, Fridlyand J, Bauer J, et al. Improving melanoma classification by integrating genetic and morphologic features. PLoS Med 2008;5(6):e120.
25. Long GV, Menzies AM, Nagrial AM, et al. Prognostic and clinicopathologic associations of oncogenic BRAF in metastatic melanoma. J Clin Oncol 2011;29: 1239-46.
26. Phadke PA, Zembowicz A. Blue nevi and related tumors. Clin Lab Med 2011; 31:345-58.
27. Chen LL, Jaimes N, Barker CA, Busam KJ, Marghoob AA. Desmoplastic melanoma: a review. J Am Acad Dermatol 2013; 68:825-33.
28. Shain AH, Garrido M, Botton T, et al. Exome sequencing of desmoplastic melanoma identifies recurrent NFKBIE promoter mutations and diverse activating mutations in the MAPK pathway. Nat Genet 2015 September 7 (Epub ahead of print).
29. Rivers JK. Is there more than one road to melanoma? Lancet 2004;363:728-30.
30. Whiteman DC, Watt P, Purdie DM, Hughes MC, Hayward NK, Green AC. Melanocytic nevi, solar keratoses, and divergent pathways to cutaneous melanoma. J Natl Cancer Inst 2003;95:806-12.
31. Maldonado JL, Fridlyand J, Patel H, et al. Determinants of BRAF mutations in primary melanomas. J Natl Cancer Inst 2003;95:1878-90.
32. Elder DE, Goldman LI, Goldman SC, Greene MH, Clark WH Jr. Dysplastic nevus syndrome: a phenotypic association of sporadic cutaneous melanoma. Cancer 1980;46:1787-94.
33. Tucker MA, Halpern A, Holly EA, et al. Clinically recognized dysplastic nevi: a central risk factor for cutaneous melanoma. JAMA 1997;277:1439-44.
34. Goldgar DE, Cannon-Albright LA, Meyer LJ, Piepkorn MW, Zone JJ, Skolnick MH. Inheritance of nevus number and size in melanoma and dysplastic nevus syndrome kindreds. J Natl Cancer Inst 1991;83:1726-33.
35. Gorgoulis VG, Vassiliou L-VF, Karakaidos P, et al. Activation of the DNA damage checkpoint and genomic instability in human precancerous lesions. Nature 2005;434:907-13.
36. MacKie RM, English J, Aitchison TC, Fitzsimons CP, Wilson P. The number and distribution of benign pigmented moles (melanocytic naevi) in a healthy British population. Br J Dermatol 1985;113:167-74.